Soft Matter

PAPER

View Article Online
View Journal | View Issue

Cite this: *Soft Matter*, 2015, **11**, 6235

The swim force as a body force

Wen Yan*[a] and John F. Brady[b]

Received 29th May 2015,
Accepted 2nd July 2015

DOI: 10.1039/c5sm01318f

www.rsc.org/softmatter

Net (as opposed to random) motion of active matter results from an average swim (or propulsive) force. It is shown that the average swim force acts like a body force – an internal body force. As a result, the particle-pressure exerted on a container wall is the sum of the swim pressure [Takatori *et al.*, *Phys. Rev. Lett.*, 2014, **113**, 028103] and the 'weight' of the active particles. A continuum description is possible when variations occur on scales larger than the run length of the active particles and gives a Boltzmann-like distribution from a balance of the swim force and the swim pressure. Active particles may also display 'action at a distance' and accumulate adjacent to (or be depleted from) a boundary without any external forces. In the momentum balance for the suspension – the mixture of active particles plus fluid – only external body forces appear.

1 Introduction

The soft matter community has proposed several theoretical approaches to investigate the behavior of active matter systems. Thermodynamic-type models, such as the ϕ^4 field theory,[1] motility-induced-phase-separation,[2,3] and density functional theory,[4] treat active matter as a single substance and try to fit it into the classical framework of the states of matter. For example, the dilute-dense coexistence of active matter can be formulated as a first-order gas–liquid phase transition.[5,6]

Despite its success in explaining some states of active soft matter, thermodynamic models are not sufficient when the detailed dynamics, structure and deformation are of interest, especially when external perturbations are applied. In these situations, Fokker–Planck or Smoluchowski equations are often used as they directly relate the individual swimmer's Langevin equation to the position-orientation $(\boldsymbol{x},\boldsymbol{q})$ phase space probability density $P(\boldsymbol{x},\boldsymbol{q},t)$, which gives all the detailed information of interest. Active matter under an external force,[7] polarization,[8] and rectification[9] have been investigated with this approach. When the detailed chemical propulsion mechanism or hydrodynamic interaction are considered, $P(\boldsymbol{x},\boldsymbol{q},t)$ can be solved together with the conservation equation for chemical species concentration $c(\boldsymbol{x},t)$ or the flow field $\boldsymbol{u}(\boldsymbol{x},t)$, allowing detailed knowledge of the dynamics, such as the system's stability.[10]

The Smoluchowski approach, however, is not able to treat concentrated systems where particle–particle interactions are important, even for the simplest excluded volume interactions. For dense active matter, simulation is the standard approach. Active Brownian dynamics simulations of as many as 10^7 particles have been reported in order to investigate phase behavior.[11] A few simulations of active matter with hydrodynamic interactions have also been reported.[12,13]

Even with a wealth of simulation data, some fundamental questions remain. For example, how does one predict the force exerted on a boundary by (dense) active matter? Simulations give an *a posterior* determination of the force,[14,15] while the Smoluchowski approach can be used but only for dilute systems when particle–particle interactions are ignored.[16]

For conventional atomic or molecular matter, at the particle level there are Newton's laws of motion and their phase-space equivalent the Liouville equation. For active colloids, the corresponding particle-level equations are the Langevin equation and the Smoluchowski equation. Thermodynamics, whether for conventional or active matter, does not permit any spatial or temporal variation in properties and thus, while powerful, has its limitations. To bridge the gap between the detailed particle and the thermodynamic levels, conventional matter employs continuum mechanics which applies out of equilibrium for slow spatial and temporal variations. The purpose of this work is to investigate and develop an analogous continuum mechanics description for active matter.

In conventional matter, forces at the particle level do not manifest themselves in the continuum momentum balance unless they are external body forces. Interparticle forces contribute to the continuum stress, but do not act as net forces at the continuum level. For active matter the situation is more complex and more interesting. As we show, the propulsive swim force acting at the particle level that causes particles to move is part of the hydrodynamic force the particles exert on the fluid,

[a] *Department of Mechanical & Civil Engineering, California Institute of Technology, Pasadena, CA 91125, USA. E-mail: wyan@caltech.edu*
[b] *Division of Chemistry & Chemical Engineering and Engineering & Applied Science, California Institute of Technology, Pasadena, CA 91125, USA. E-mail: jfbrady@caltech.edu*

and thus when considering the momentum balance for the suspension – the mixture of particles plus fluid – there is no net hydrodynamic force and thus no net swim force acting on the mixture; only external body forces appear. However, the suspension is a two-phase mixture of active particles and fluid and in the continuum momentum balance for the particle phase we show that a net swim force appears directly and acts as an internal body force. This net swim force is crucial for describing the dynamics of active matter and for computing forces exerted on boundaries.

The swim force plays a pivotal role in the swim pressure,[5] whose introduction provided a new approach to understanding the behavior of active matter. Active Brownian particles (ABPs) that separate into dilute and dense regions are now understood as a 'gas–liquid' coexistence. The decrease in the swim pressure with concentration destabilizes the system resulting in phase separation.[5,6] The swim pressure is analogous to the osmotic pressure of a chemical solute or of passive Brownian particles and is the pressure needed to confine the active particles. In the dilute limit the ''ideal gas'' swim pressure is $\Pi^{\mathrm{swim}} = n\zeta U_0{}^2\tau_{\mathrm{R}}/6$ (in 3D), where n is the number density of active particles, ζ is their drag coefficient, U_0 is the swim speed, and τ_{R} is their reorientation time.[5]

While the swim pressure can be understood solely in terms of this entropic confinement pressure and is independent of the size of the swimmers,[5] micromechanically, the swim stress is given by the moment of the swim force $\langle\boldsymbol{\sigma}^{\mathrm{swim}}\rangle = -n\langle\boldsymbol{x}\boldsymbol{F}^{\mathrm{swim}}\rangle$, where $\boldsymbol{F}^{\mathrm{swim}} = \zeta U_0\boldsymbol{q}$, with $\boldsymbol{q}$ the orientation vector of the swimmer and $\boldsymbol{x}$ its position. The position is simply $\boldsymbol{x}(t) = \int^t U_0\boldsymbol{q}(t')\mathrm{d}t'$, and thus, $\sigma^{\mathrm{swim}} = -n\zeta U_0{}^2\int^t\langle\boldsymbol{q}(t)\boldsymbol{q}(t')\rangle\mathrm{d}t' = -n\zeta U_0{}^2\tau_{\mathrm{R}}/6\boldsymbol{I}$ (for times $t \gg \tau_{\mathrm{R}}$), arising from the random reorientation of the swimmer: $\langle\boldsymbol{q}(t)\boldsymbol{q}(t')\rangle = (\boldsymbol{I}/3)\exp\{-2(t-t')/\tau_{\mathrm{R}}\}$. The 'moment arm' for the swim stress is the swimmer's run length, $\ell = U_0\tau_{\mathrm{R}}$.

The micromechanical definition of the swim stress thus involves the swim force, which leads to questions about the 'force-free' nature of low-Reynolds number swimming. Furthermore, the swim stress sparked some recent discussion[17] about whether it is a true stress – is it equal to the force per unit area on the bounding walls? – especially when the dynamics give rise to polar order: a non-zero average orientation of the particles, $\langle\boldsymbol{q}\rangle \neq 0$.

In this paper we first show the origin and definition of the swim force that is consistent with the notion of 'force-free' motion. We then establish the global force (or momentum) balance for active matter, focusing on the case when there is net polar order $\langle\boldsymbol{q}\rangle$, which corresponds to an average swim force $\langle\boldsymbol{F}^{\mathrm{swim}}\rangle$. We show that in the momentum balance for the active particles, the average swim force acts just like a body force, with the result that the force/area exerted by active matter on a bounding wall is the sum of the swim pressure and the 'weight' of the active particles. Thus, the questions raised in Solon *et al.*[18] are straightforwardly resolved and in a manner completely consistent with one's intuition about forces and pressures.

Further, we show that a sedimentation-like system is achieved for $\langle\boldsymbol{F}^{\mathrm{swim}}\rangle \neq 0$ without any external body force and a continuum Boltzmann distribution holds just as for passive Brownian particles in a gravitational field. Active particles may also accumulate adjacent to (or be depleted from) a boundary, for example in response to an external stimulus (chemical, light, *etc.*). The interesting aspect is that this accumulation (depletion) occurs without there being any external force acting on the particles; it is a true 'action at a distance'.

Although an average swim force acting like a body force arises naturally from the particle-level dynamics, it is nevertheless surprising since, as mentioned before, it does not appear in the macroscopic momentum balance for the entire suspension, or mixture, of particles plus fluid.

2 The swim force

In self-propulsion at low Reynolds number by 'force-free' one means that there is no external force causing the body to move. The '*internal*' forces that cause it to move arise from deformation of the body surface and are part of the total hydrodynamic force (and torque), which, from the linearity of Stokes flow, can be written as

$$\begin{aligned}\mathscr{F}^{\mathrm{H}} &= -\underbrace{\boldsymbol{R}_{\mathscr{F}\mathscr{U}}\cdot\mathscr{U}} - \underbrace{\boldsymbol{R}_{\mathscr{F}E} : \boldsymbol{E}^{\mathrm{s}} - \boldsymbol{R}_{\mathscr{F}B}\odot\boldsymbol{B}^{\mathrm{s}} - \cdots} \\ &= \quad \mathscr{F}^{\mathrm{drag}} \quad + \quad \mathscr{F}^{\mathrm{swim}},\end{aligned} \tag{1}$$

where we have grouped the force/torque together as a single vector, $\mathscr{F}^{\mathrm{H}} = (\boldsymbol{F}^{\mathrm{H}},\boldsymbol{L}^{\mathrm{H}})$, and similarly for the translational/rotational velocities: $\mathscr{U} = (\boldsymbol{U},\boldsymbol{\Omega})$. The hydrodynamic tensors $\boldsymbol{R}_{\mathscr{F}\mathscr{U}}$, $\boldsymbol{R}_{\mathscr{F}E}$, *etc.* are functions of the body geometry only and couple the force to the velocity, to the 'squirming set' $\boldsymbol{E}^{\mathrm{s}}(t)$, $\boldsymbol{B}^{\mathrm{s}}(t)$, *etc.*, which characterize the 'slip' velocity at the body surface. A derivation of (1) can be found in Appendix A.

In (1) the hydrodynamic force/torque is written as a sum of two terms: (i) the hydrodynamic drag $\mathscr{F}^{\mathrm{drag}}$ and (ii) the propulsive or 'swim' force $\mathscr{F}^{\mathrm{swim}}$. Eqn (1) provides the definition of the swim force. That it is a real measurable force can be appreciated by recognizing that if one wanted to keep the swimmer from moving, say by trapping it with optical tweezers, the force/torque the trap would exert is precisely $\mathscr{F}^{\mathrm{swim}}$.

In addition to the hydrodynamic drag and swim force, active particles can also be subject to thermal Brownian motion ($\mathscr{F}^{\mathrm{B}} = 2k_{\mathrm{B}}T\boldsymbol{R}_{\mathscr{F}\mathscr{U}}\delta(t)$), external forces such as buoyancy ($\mathscr{F}^{\mathrm{ext}}$), and interparticle forces, for example repulsive interactions to prevent overlap at finite concentrations ($\mathscr{F}^{\mathrm{P}}$).†

In the simplest model of active particles the hydrodynamic resistance tensor is an isotropic drag tensor $\boldsymbol{R}_{\mathrm{FU}} = \zeta\boldsymbol{I}$ and the swim force is $\boldsymbol{F}^{\mathrm{swim}} = \zeta U_0\boldsymbol{q}$. This is the 'Active Brownian Particle' (ABP) model:

$$0 = -\zeta\boldsymbol{U} + \boldsymbol{F}^{\mathrm{swim}} + \boldsymbol{F}^{\mathrm{B}} + \boldsymbol{F}^{\mathrm{ext}} + \boldsymbol{F}^{\mathrm{P}}. \tag{2}$$

The orientation vector $\boldsymbol{q}$ is subject to run-and-tumble or rotational Brownian diffusion ($D_{\mathrm{R}} = 1/\tau_{\mathrm{R}}$), which are equivalent,[19] and follows directly from the torque balance. For a spherical swimmer, $\zeta = 6\pi\eta a$, where a is the particle size and η the

† Hydrodynamic shear forces can also be present, but are not considered here; they enter in eqn (1).

viscosity of the suspending Newtonian fluid. A more detailed derivation of (2) can be found in Appendix A.

In this paper we focus on the ABP model (eqn (2)), with both translational and rotational diffusion: D_T, D_R. The reorientation time is $\tau_R = 1/D_R$. The relative importance of advection by swimming to translational swim diffusion is given by the reorientation Péclet number[5] $\mathrm{Pe}_R = U_0 a/(6D^{\mathrm{swim}}) = a/U_0\tau_R$, and is also the ratio of the particle size to the swimmer's run length.

3 The global force balance

Consider a very simple geometry where N swimmers are placed between two parallel walls separated by a distance L whose normals are along the z-direction as illustrated in Fig. 1. The walls are of large extent (infinite) and system can be taken to be periodic in the x- and y-directions. The walls are non-penetrating to swimmers but allow the solvent to pass through unimpeded – they are osmotic barriers. Each swimmer i experiences a wall force $\boldsymbol{F}_i^{\mathrm{W}}$ when it 'collides' with a wall. The separation L between the walls is sufficiently large so that the swimmers are able to execute their random swim motion before colliding with the walls – the swimmer's size a and run length ℓ are both small compared to L.

The global force balance is the sum over all swimmers of each individual Langevin eqn (2). At steady state $\sum_i \boldsymbol{U}_i = 0$ and

$$0 = N\zeta U_0\langle \boldsymbol{q}\rangle + N\langle \boldsymbol{F}^{\mathrm{ext}}\rangle + \boldsymbol{F}^{\mathrm{W}}_{\mathrm{Top}} + \boldsymbol{F}^{\mathrm{W}}_{\mathrm{Bot}}, \qquad (3)$$

where $\langle \boldsymbol{q}\rangle = \frac{1}{N}\sum_i \boldsymbol{q}_i$, $\langle \boldsymbol{F}^{\mathrm{ext}}\rangle = \frac{1}{N}\sum_i \boldsymbol{F}_i^{\mathrm{ext}}$, and $\boldsymbol{F}^{\mathrm{W}}_{\mathrm{Top}} = \sum_{i\in T} \boldsymbol{F}_i^{\mathrm{W}}$ is the force on the top wall and involves only those particles interacting with that wall; a similar expression applies to the bottom wall.

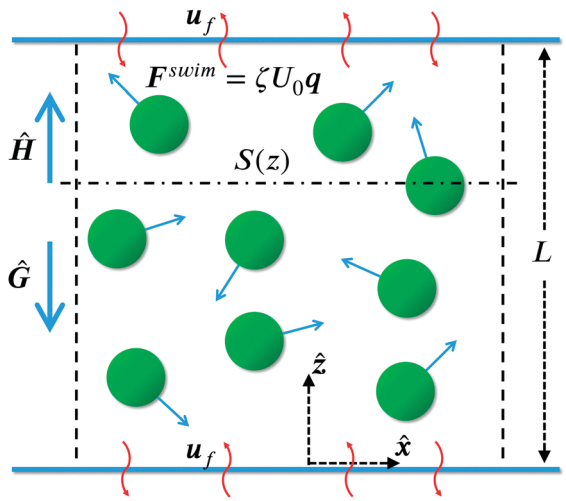

Fig. 1 Active Brownian particles (ABPs) in a container of height L in the z-direction and periodic in the x- and y-directions. Each active particle experiences a swim force $\boldsymbol{F}^{\mathrm{swim}} = \zeta U_0 \boldsymbol{q}$, with $\boldsymbol{q}(t)$ the direction of swimming. An external gravitational ($\hat{\boldsymbol{G}}$) and polarization ($\hat{\boldsymbol{H}}$) field may also be applied. The top and bottom boundaries do not allow the particles to escape (no flux), but the flow of fluid $\boldsymbol{u}_f$ is unimpeded – they are osmotic barriers. The horizontal plane $S(z)$ is the cross-section considered in global force balance (4).

The Brownian and interparticle forces in (2) make no contribution to the global balance. Brownian forces, by definition, have zero average, while the interparticle forces are equal and opposite when two particles interact.

The net force on the walls is balanced by the total external body force acting on the particles within the volume plus the total average swim force. As far as the particles are concerned, an average swim force, $\langle \boldsymbol{F}^{\mathrm{swim}}\rangle = \zeta U_0\langle \boldsymbol{q}\rangle$, acts like just like a body force – an internal body force.

Now consider a control volume composed of the bottom wall and a horizontal plane at an arbitrary location z above the wall (*cf.* Fig. 1). The global force balance is

$$0 = \int_{V(z)} \left(\boldsymbol{F}^{\mathrm{swim}} + \boldsymbol{F}^{\mathrm{ext}}\right)\mathrm{d}V + \boldsymbol{F}^{\mathrm{W}}_{\mathrm{Bot}} + \int_{S(z)} \sigma^{(\mathrm{p})}\cdot \boldsymbol{n}\mathrm{d}S, \qquad (4)$$

where $S(z)$ is the horizontal surface at z and $\boldsymbol{\sigma}^{(\mathrm{p})}$ is the force per unit area or stress exerted on the material (*i.e.* particles) within the control volume. (There is no contribution from the surfaces in the x- and y-directions because of the assumed periodicity.)

The surface $S(z)$ is of large horizontal extent and therefore forms an average. If the variation in properties in the z-direction is slow on the scale of the particle size and/or run length, we may replace the surface stress with the particle-phase stress (at z) found by standard averaging of the microscale dynamics (2) *viz.*:

$$\langle \boldsymbol{\sigma}^{(\mathrm{p})}\rangle = -nk_{\mathrm{B}}T\boldsymbol{I} - n\langle \boldsymbol{x}(\boldsymbol{F}^{\mathrm{swim}})'\rangle - n\langle \boldsymbol{x}\boldsymbol{F}^{\mathrm{P}}\rangle, \qquad (5)$$

where the first term on the RHS is the ideal gas Brownian osmotic pressure and the last term is the collisional pressure from the interactive forces. For the swim stress, the average swim force must be removed when computing the stress: $(\boldsymbol{F}^{\mathrm{swim}})' = \boldsymbol{F}^{\mathrm{swim}} - \langle \boldsymbol{F}^{\mathrm{swim}}\rangle$.

The z-component of the force balance in (4) is

$$\Pi^{\mathrm{W}}_{\mathrm{Bot}} = \Pi^{(\mathrm{p})}(z) - \int_0^z \left(n\langle F_z^{\mathrm{ext}}\rangle + n\langle F_z^{\mathrm{swim}}\rangle\right)\mathrm{d}z, \qquad (6)$$

where $\Pi^{\mathrm{W}}_{\mathrm{Bot}} = F_z^{\mathrm{W}}/A$ is the pressure on the bottom wall of area A, $\Pi^{(\mathrm{p})}$ is the pressure of the active suspension at z, and the averages under the integral sign are number averages in the horizontal plane. The force balance (6) requires no knowledge of the distribution of active particles $n(z)$, nor how or why there may be an average swim force. The pressure on the wall differs from the pressure of the active particles if there is a body force – external or internal – acting on the particles. Indeed, in general, if the pressure differs between two horizontal planes, then either (i) the material between the planes must be accelerating, or (ii) the pressure difference must be balanced by shear stresses at the boundaries as in flow in a tube, or (iii) there must be body forces acting throughout the volume.

The effect of an external body force is well-known, and our derivation shows that an average swim force has the same effect. An average swim force could exist throughout the volume if the swimmers had a biased swimming, say due to a gradient in a stimulant (chemical, light, *etc.*), or it can arise from the boundary if the boundary were to promote a local orientational order.

Recently, Solon *et al.*[18] derived the dilute limit expression for the wall pressure when an external torque is applied to each

ABP that collides with the wall and found that Π^{W} depends on the form of the torque and therefore concluded that the swim pressure was ill-defined because, according to them, it depended on the nature of the wall and therefore was not a 'true' pressure. A nonzero torque induces a local $\langle \boldsymbol{q} \rangle$ and therefore a nonzero swim force that must be included in the momentum balance. When this internal body force is included the global force balance (6) is satisfied and the swim pressure is indeed well-defined and independent of the boundaries.‡

4 Particle-phase momentum balance

Straightforward averaging of the microscale dynamics (2) results in the momentum balance for the particle phase:

$$0 = -\zeta \langle \boldsymbol{j}^{\mathrm{rel}} \rangle + n \langle \boldsymbol{F}^{\mathrm{swim}} \rangle + n \langle \boldsymbol{F}^{\mathrm{ext}} \rangle + \nabla \cdot \langle \boldsymbol{\sigma}^{(\mathrm{p})} \rangle. \qquad (7)$$

In (7) $\langle \boldsymbol{j}^{\mathrm{rel}} \rangle = n(\langle \boldsymbol{u}_{\mathrm{p}} \rangle - \langle \boldsymbol{u} \rangle)$ is the particle flux relative to the suspension average velocity. Here, $\langle \boldsymbol{u}_{\mathrm{p}} \rangle = \frac{1}{N} \sum_i \boldsymbol{U}_i$, and $\langle \boldsymbol{u} \rangle = \phi \langle \boldsymbol{u}_{\mathrm{p}} \rangle + (1 - \phi) \langle \boldsymbol{u}_{\mathrm{f}} \rangle$, with ϕ the volume fraction of particles and $\langle \boldsymbol{u}_{\mathrm{f}} \rangle$ the average fluid velocity. Eqn (7) should apply locally at each 'continuum point', provided, as is standard in any continuum description, that there is a separation in scales with the macroscopic variations occurring on scales large compared to the microstructural length scales, importantly the run length $\ell = U_0 \tau_{\mathrm{R}}$.

The momentum balance is used with the conservation of particle number density:

$$\frac{\partial n}{\partial t} + \nabla \cdot \langle \boldsymbol{u} \rangle n + \nabla \cdot \langle \boldsymbol{j}^{\mathrm{rel}} \rangle = 0, \qquad (8)$$

to determine the spatial distribution of active particles. In general, an equation for the orientation distribution $\langle \boldsymbol{q} \rangle$ is needed, which can be found from the Smoluchowski equation equivalent to the microscale dynamics (2). In the problems discussed here it is not needed.

The global force balance, (3) or (4), applies quite generally. In contrast, the continuum mechanics description, (7) and (8), requires a separation of scales between the microscale and the macroscale. While this separation is almost always true for passive Brownian particles, it requires careful examination for active matter, which we address in a future study.[20]

This completes the general discussion of the balance laws for active particles. We now demonstrate by a few illustrative examples that the average swim force acts as an internal body force and that the particle-phase momentum balance can accurately predict the concentration distributions and the forces on the walls.

5 The effect of internal and external body forces

5.1 Passive particles with gravity

We first consider a suspension of passive Brownian particles in a container as illustrated in Fig. 1. The swim force is zero, $\boldsymbol{F}^{\mathrm{swim}} = 0$, and, when dilute, the particle phase stress is simply the Brownian osmotic pressure $\langle \boldsymbol{\sigma}^{(\mathrm{p})} \rangle = -n k_{\mathrm{B}} T \boldsymbol{I}$; the collisional stress is $O(n^2)$. In the absence of gravity, the number density is uniform with height $n(z) = n_0$ and the pressure on walls from (6) is the osmotic pressure $\Pi^{\mathrm{W}}_{\mathrm{Bot}} = \Pi^{\mathrm{W}}_{\mathrm{Top}} = n_0 k_{\mathrm{B}} T$. With gravity, $\boldsymbol{F}^{\mathrm{ext}} = \Delta\rho V_{\mathrm{p}} \boldsymbol{g}$; the buoyant force is given by the density difference $\Delta\rho = \rho_{\mathrm{p}} - \rho_{\mathrm{f}}$ times the volume of a particle V_{P} and the acceleration of gravity $\boldsymbol{g}$. The passive Brownian particles behave like an isothermal ideal gas in an external potential. At steady state there is no suspension velocity, $\langle \boldsymbol{u} \rangle = 0$, and the particles cannot escape the container, $\langle \boldsymbol{j}^{\mathrm{rel}} \rangle = 0$. From (7) in the dilute limit, $n(z)$ has a Boltzmann distribution: $n(z) = n_0 (L/L_{\mathrm{G}}) \exp(-z/L_{\mathrm{G}}) / (1 - \exp(-L/L_{\mathrm{G}}))$, where $L_{\mathrm{G}} = k_{\mathrm{B}} T / \Delta\rho V_{\mathrm{p}} g$ is the sedimentation length. The pressures at the walls are $\Pi^{\mathrm{W}}_{\mathrm{Bot}} = n(z = 0) k_{\mathrm{B}} T$ and $\Pi^{\mathrm{W}}_{\mathrm{Top}} = n(z = L) k_{\mathrm{B}} T$, and their difference, $\Pi^{\mathrm{W}}_{\mathrm{Bot}} - \Pi^{\mathrm{W}}_{\mathrm{Top}} = n_0 \Delta\rho V_{\mathrm{p}} g L$, is the total buoyant weight of the particles in the container, in agreement with the global force balance (6).

5.2 Active particles with gravity

We now examine a similar system of swimmers (ABPs) under gravity. Provided the gravitational forcing is not too strong no polar order will be induced by the no flux boundary at the bottom.[7,9,20,21] In 2D for a dilute system the swim stress $\langle \boldsymbol{\sigma}^{\mathrm{swim}} \rangle = -n\zeta {U_0}^2 \tau_{\mathrm{R}} / 2 \boldsymbol{I}$, and the total particle-phase stress is $\langle \boldsymbol{\sigma}^{(\mathrm{p})} \rangle = -n(k_{\mathrm{B}} T + k_{\mathrm{s}} T_{\mathrm{s}}) \boldsymbol{I}$, where we define the swimmer 'activity' $k_{\mathrm{s}} T_{\mathrm{s}} \equiv \zeta {U_0}^2 \tau_{\mathrm{R}} / 2$. We perform active Brownian dynamics simulations in 2D with periodic boundary conditions in x and with a hard-particle potential when particles collide with each other or with either the top or bottom walls. Eqn (7) predicts a Boltzmann distribution: $n(z) \propto \exp(-\Delta\rho V_{\mathrm{p}} g z / (k_{\mathrm{B}} T + k_{\mathrm{s}} T_{\mathrm{s}}))$ in the dilute limit, which is verified by simulation over a wide range of (dilute) area fractions $\phi^0_{\mathrm{A}} = n_0 \pi a^2$, reorientation Péclet numbers $\mathrm{Pe}_{\mathrm{R}} = a / (U_0 \tau_{\mathrm{R}}) \in (0.2, 5.0)$, with or without translational diffusion, D_{T}, and not too large gravity ($\Delta\rho V_{\mathrm{p}} g / (\zeta U_0) < 0.2$) as shown in Fig. 2. The global force balance (3) (and (6)) is verified by measurement of the force on the bottom wall in the simulations.

5.3 Orienting field to cancel gravity

From the global force balance (3), if $\langle \boldsymbol{F}^{\mathrm{ext}} \rangle$ and $\langle \boldsymbol{F}^{\mathrm{swim}} \rangle$ cancel each other, then $\Pi^{\mathrm{W}}_{\mathrm{Bot}} = \Pi^{\mathrm{W}}_{\mathrm{Top}}$ and the continuum theory (7) predicts a uniform distribution of active particles. To test this, a non-zero $\langle \boldsymbol{q} \rangle$ can be induced by an external polarization field as discussed by Takatori and Brady.[8] An external field $\hat{\boldsymbol{H}}$ applies a torque $\Omega_{\mathrm{c}} \boldsymbol{q} \times \hat{\boldsymbol{H}}$ to each swimmer and therefore the orientation vector $\boldsymbol{q}$ aligns in the field direction and diffuses around it through $D_{\mathrm{R}} = 1/\tau_{\mathrm{R}}$. The strength of the applied field is governed by the nondimensional field strength $\chi_{\mathrm{R}} = \Omega_{\mathrm{c}} \tau_{\mathrm{R}}$. When $\chi_{\mathrm{R}} \to 0$ the structure is isotropic, whereas when $\chi_{\mathrm{R}} \to \infty$ all particles align and move in the direction $\hat{\boldsymbol{H}}$. Each swimmer has a net average velocity $U_0 \langle \boldsymbol{q} \rangle (\chi_{\mathrm{R}})$ due to the field, which can be canceled by $\boldsymbol{F}^{\mathrm{ext}} / \zeta$. With an orienting field the swim stress is anisotropic and given in ref. 8 in 3D and in Appendix B for 2D.

Simulations were conducted in the same bounded geometry with $\hat{\boldsymbol{H}}$ and gravity both perpendicular to the walls for a wide range of χ_{R} and $\boldsymbol{F}^{\mathrm{ext}}$. The systems are homogeneous at steady

‡ The body force contribution is identical to the second term in eqn (7) of Solon *et al.*[18]

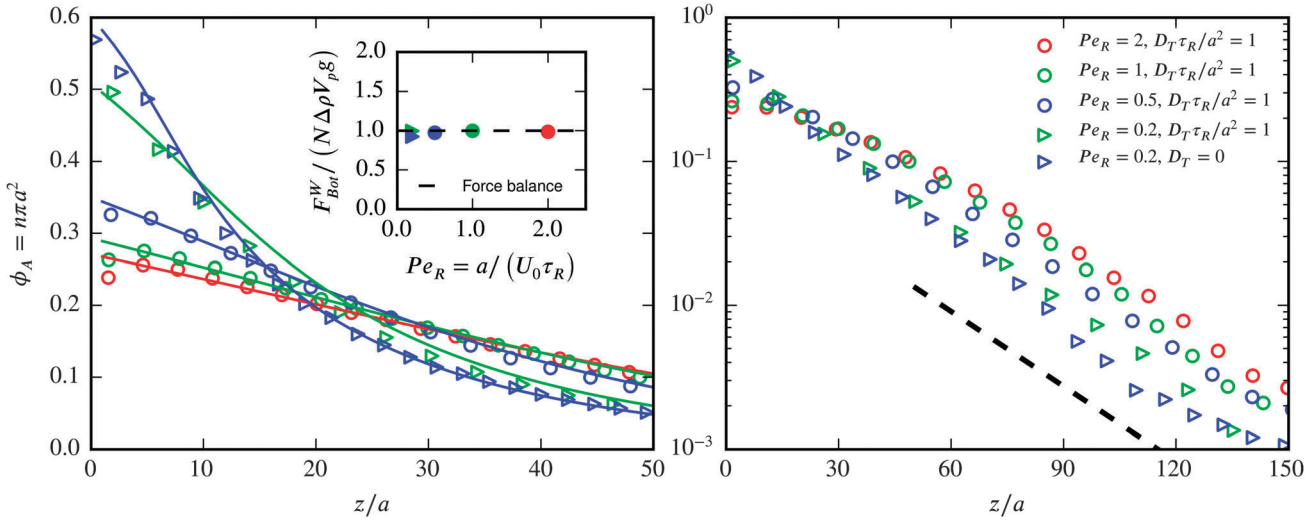

Fig. 2 Active particles with gravity. The local area fraction ϕ_A *vs.* height z/a in 2D. The symbols are simulation results and the solid lines are solutions to the continuum description (7). The log plot shows the same data as the linear plot. The dashed line corresponds to Boltzmann distribution $n \propto \exp(-\Delta\rho V_p g z/(k_B T + k_s T_s)) = \exp(-0.04z/a)$; here $k_s T_s = \zeta U_0^2 \tau_R/2$. $N = 1000$ particles are simulated in a square box of size $250a$, and $\phi_A^0 = 0.05$. The box is periodic in the x-direction but confined by two no-flux walls located at $z = 0$ and $z = L$. The inset compares the force on the bottom wall from the particle–wall interactions in simulation with the buoyant weight of the particles.

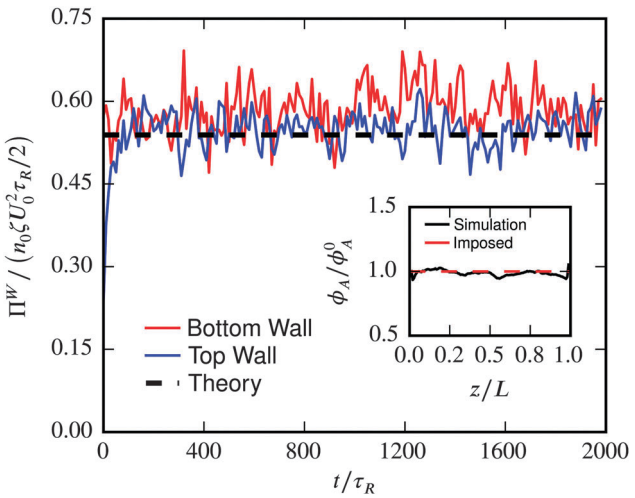

Fig. 3 Orienting field to cancel gravity. The wall pressure *vs.* simulation time. Here, $Pe_R = a/(U_0\tau_R) = 0.2$, $D_T = 0$, $\chi_R = \Omega_c\tau_R = 1$ and $\Delta\rho V_P g\tau_R/(\zeta a) = 2.23 = \langle q_z\rangle U_0\tau_R/a$. The inset shows the local area fraction ϕ_A as a function of height z, sampled by Voronoi cells. $N = 1668$ particles are simulated in a square box of size $512a$ at $\phi_A^0 = 0.02$. The data are averaged over 16 realizations. The system is periodic in the x-direction but confined by two no-flux walls located at $z = 0$ and $z = L$. The theory for the dilute limit and can be found in Appendix B.

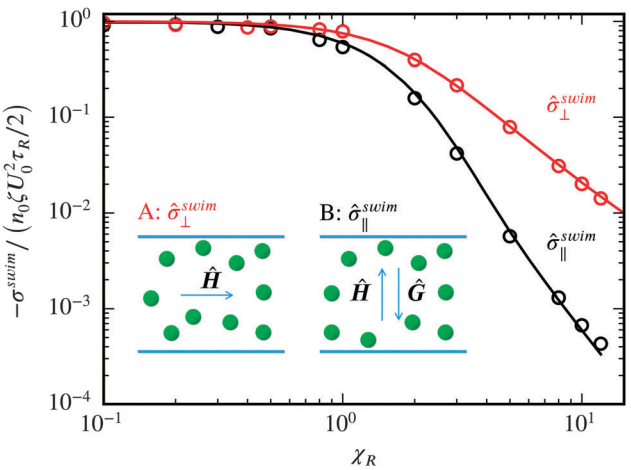

Fig. 4 The anisotropic wall pressures compared with the dilute 2D theory (Appendix B). The circles are ABP simulations for $Pe_R = a/(U_0\tau_R) = 0.2$, $D_T = 0$, $\phi_A^0 = 0.02$ and $N = 1668$. (A) for $\hat{\sigma}_\perp$ the $\hat{\boldsymbol{H}}$ field is applied in x-direction, whereas (B) for $\hat{\sigma}_\parallel$ the $\hat{\boldsymbol{H}}$ is applied in the z-direction and canceled by $\boldsymbol{F}^{ext}$. The square box of size $512a$ is periodic in x and confined by no-flux walls located at $z = 0$ and $z = L$.

state when gravity cancels the field (Fig. 3), and the wall pressures are equal as the global force balance (3) requires.

Theory[8] predicts anisotropic stresses, and simulations were conducted at low area fraction ($\phi_A \approx 0.02$) without translational Brownian motion so that $\langle\boldsymbol{\sigma}^{(p)}\rangle = nk_sT_s(\hat{\sigma}_\parallel^{swim}\hat{\boldsymbol{H}}\hat{\boldsymbol{H}} + \hat{\sigma}_\perp^{swim}(\boldsymbol{I} - \hat{\boldsymbol{H}}\hat{\boldsymbol{H}}))$, where $\hat{\sigma}_\parallel^{swim}$ and $\hat{\sigma}_\perp^{swim}$ are nondimensional functions of χ_R. To measure $\hat{\sigma}_\perp^{swim}$, the $\hat{\boldsymbol{H}}$ field is applied parallel to the walls (case A in Fig. 4); and for $\hat{\sigma}_\parallel^{swim}$, $\hat{\boldsymbol{H}}$ and the gravity field are perpendicular to the walls and cancel each other (case B in Fig. 4). Fig. 4 shows that the pressures on the walls determined in simulation agree with the theory.

5.4 No gravity but with an orienting field

The resemblance of a swim force to an external body force is further illustrated by a system under a polarization field but no gravity. A constant downward $\hat{\boldsymbol{H}}$ field gives a 'sedimentation-like' system with swimmers accumulating near the bottom wall as shown in Fig. 5. The measured bottom wall pressure is equal to the total 'weight' of the particles (divided by length L_x in 2D): $N\langle F^{swim}\rangle/L_x$, as the global force balance (3) requires. Solving (7)

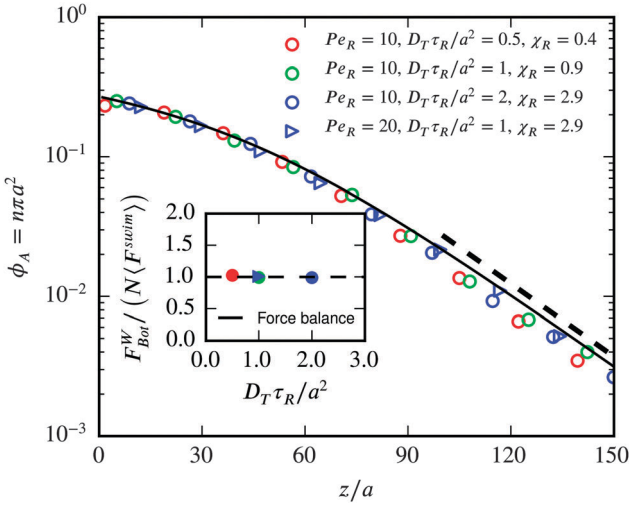

Fig. 5 No gravity but with an orienting field. The local area fraction ϕ_A *vs.* height z/a with the $\hat{\boldsymbol{H}}$ field applied downward and $\boldsymbol{F}^{ext} = 0$. The symbols are simulation results and the solid line is the solution to the continuum description (7). The dashed line is a Boltzmann distribution $\phi_A \propto \exp\{-\langle \boldsymbol{F}^{swim}\rangle z/(k_BT + k_sT_s\hat{\sigma}_{\parallel})\} = \exp(-0.04z/a)$, where $k_sT_s = \zeta U_0{}^2\tau_R/2$. $N = 1000$ particles are simulated in a square box of size $250a$ at $\phi_A^0 = 0.05$. The box is periodic in x but confined by no-flux walls at $z = 0$, L. The inset compares the force on the bottom wall from the particle–wall interactions in simulation with the 'weight' of the particles due to the swim force.

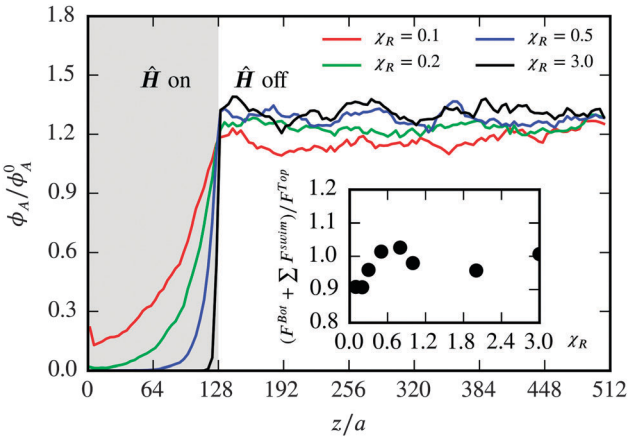

Fig. 6 A depletion zone induced by polarization. The local area fraction ϕ_A *vs.* height z/a with the $\hat{\boldsymbol{H}}$ field applied upward in the region $z < L/4$ and $\boldsymbol{F}^{ext} = 0$. The solid lines are simulation. $N = 1668$ particles are simulated in a square box of size $512a$ at $\phi_A^0 = 0.02$. The box is periodic in x but confined by no-flux walls at $z = 0$, L. $Pe_R = 0.2$, $D_T = a^2/\tau_R$. The inset checks the global force balance (3) and (4).

with $\langle \boldsymbol{F}^{swim}\rangle = \zeta U_0\langle \boldsymbol{q}\rangle(\chi_R)$ gives a Boltzmann distribution where the concentration is dilute with the 'sedimentation length' $L_{\parallel} = (k_BT + k_sT_s\hat{\sigma}_{\parallel}^{swim})/\langle F^{swim}\rangle$. The only difference compared to normal gravity is the anisotropic swim stress manifested by $\hat{\sigma}_{\parallel}^{swim}$. As shown in Fig. 5 the calculated Boltzmann distribution $n \propto \exp(-z/L_{\parallel})$ agrees with the simulations. In the simulations shown in Fig. 5, χ_R is adjusted according to (24), covering the range $\chi_R \in (0,3)$.

Comparing the $n(z)$ distributions and the Π^W_{Bot} of passive Brownian particles (Fig. 2) with swimmers under gravity (Fig. 5), one sees clearly that with a non-zero $\langle \boldsymbol{q}\rangle$ swimmers behave as if acted upon by a body force. An internal body force $\boldsymbol{F}^{int} = \zeta U_0\langle \boldsymbol{q}\rangle = \langle \boldsymbol{F}^{swim}\rangle$ acts on each particle.

5.5 Depletion zone

Up to now we have considered the simplest cases in which polar order was induced by an orienting field homogeneously throughout the region between the two bounding walls. But this is not necessary. Suppose that the orienting field acts only over a length $\Delta < L$. The effect of this field will lead to a depletion (or an accumulation) of active particles near the boundary depending on whether the field causes the particles to swim away from or towards the boundary. If the field is strong enough, there will be no particles contacting the wall and thus Π^W_{Bot} in (6) will be zero. For $z > \Delta$ there is no field and $\langle F_z^{swim}\rangle = 0$, while for $z < \Delta$, $n \approx 0$, and since the swim pressure far from the wall is $\Pi^{(p)} = n\zeta U_0{}^2\tau_R/6$, the global force balance (6) shows that there must be a transition region of thickness $O(\ell = U_0\tau_R)$ of high concentration of active particles near Δ. A particle swimming into the exclusion region $z < \Delta$ will, for a reorientation time, be unaware of the field and continue traveling at the swim speed. Fig. 6 demonstrates this behavior where a polarization field $\hat{\boldsymbol{H}}$ is applied only in the region $z < L/4$. If the field is strong enough, $\chi_R > 1$, there are no particles adjacent to the wall.

This is a very interesting result in that there are no external forces acting on the particles, yet they move away from the wall. Passive particles cannot do this. By sensing their environment (light, chemical, *etc.* stimuli) active particles can adjust their internal swimming mechanisms and behave as if they experienced an actual repulsive (or attractive) force. Note that we modeled the orientation process as resulting from an external torque due to the field, but this is not necessary. All that is necessary is that the active particles adjust their swimming in response to their environment and they can do this completely internally by simply 'choosing' to swim towards or away from the stimulus. No external torque (or force) is needed. It is truly an 'action at a distance'.

6 Suspension momentum balance

We have discussed the global force balance for the particle phase, but have not yet addressed the macroscopic momentum balance for entire suspension, or mixture, – the particles plus the fluid. For the mixture it must be appreciated that $\boldsymbol{F}^{drag}$ and $\boldsymbol{F}^{swim}$ at the particle level are both parts of the hydrodynamic force $\boldsymbol{F}^H$ exerted by the fluid on the particles (eqn (1)). The particles in turn exert the same force on the fluid, and thus only the external body force appears in the macroscopic momentum balance for the suspension:

$$0 = n\langle \boldsymbol{F}^{ext}\rangle + \nabla\cdot\langle \boldsymbol{\sigma}\rangle. \tag{9}$$

The average suspension stress is given by

$$\langle \boldsymbol{\sigma}\rangle = -\langle p_f\rangle \boldsymbol{I} + 2\eta\langle \boldsymbol{e}\rangle + \langle \boldsymbol{\sigma}^{(p)}\rangle, \tag{10}$$

where $\langle \boldsymbol{e} \rangle = 1/2(\nabla\langle \boldsymbol{u} \rangle + (\nabla\langle \boldsymbol{u} \rangle)^{\dagger})$ is the average rate of strain tensor and $\langle p_f \rangle$ is the average pressure in the fluid.§ The fluid pressure distribution does whatever is necessary to ensure the incompressibility of the suspension average velocity, $\nabla\cdot\langle \boldsymbol{u} \rangle = 0$. For example, when polar order exactly balances gravity (Fig. 3), $\langle \boldsymbol{\sigma}^{(p)} \rangle$ is spatially constant, there is no flux of suspension ($\langle \boldsymbol{u} \rangle = 0$) or particles ($\langle \boldsymbol{j}^{rel} \rangle = 0$) and the fluid pressure gradient is equal to the external body force, $\nabla\langle p_f \rangle = n\langle \boldsymbol{F}^{ext} \rangle$.

In the case where the orienting field gave rise to a depletion zone adjacent to the bottom wall, the suspension momentum balance shows that there will be a jump in the fluid pressure across the transition region from no particles to bulk behavior of magnitude $\Delta\langle p_f \rangle = -\int^{O(\ell)} n\langle F^{swim} \rangle \mathrm{d}z$.

Computational continuum-scale studies of active suspensions[10] employ the momentum balance (9).

7 Conclusions

Interpreting an average swim force as a body force was done at two levels of description: (i) the global force balance (3), and (ii) the continuum description (7). The global force balance looks trivial because it involves only a simple sum of each swimmer's translational Langevin equation (2). The sum is performed without any knowledge of how swimmers interact with the boundary, how they orient in $\boldsymbol{q}$-space, or how they are distributed in physical space. Also, no assumption of a 'continuum' is necessary and therefore (3) is quite general.

With the continuum approach, however, the difficult problem of determining the deformation and stress of active matter is greatly simplified to solving (7) along with the conservation equation for the particle number density (8). Further, the constitutive equation for the active stress, $\langle \boldsymbol{\sigma}^{(p)} \rangle(\phi, \mathrm{Pe}_R, \ldots)$, is determined from homogeneous active matter systems[6] and can then be used to predict the behavior in inhomogeneous situations, just as is done, for example, for the Navier–Stokes equations – the viscosity is measured in a uniform simple shear flow and then used in any flow geometry no matter how complex. When $\langle \boldsymbol{F}^{swim} \rangle$, $\langle \boldsymbol{F}^{ext} \rangle$ are specified, the continuum equations are closed and the concentration and stress, $\phi(\boldsymbol{x},t)$ and $\langle \boldsymbol{\sigma}^{(p)} \rangle(\boldsymbol{x},t)$, can be determined everywhere. The force on a boundary then follows from the standard continuum expression $\int_S \langle \sigma \rangle \cdot \boldsymbol{n} \mathrm{d}S$.

The continuum description, which predicted the Boltzmann distributions for dilute systems, requires a separation of scales between the variation in macroscopic properties, such as $n(z)$, *etc.*, and the microscale, which for active matter is set by the swimmer's run length, $\ell = U_0\tau_R$ (and/or particle size a). In very dilute systems the run length can become large and if significant polar order is induced at a boundary, a continuum description may not be possible. In a future study[20] we show how to accommodate these 'non-continuum' effects in the description of active matter.

§ There may also be a hydrodynamic stresslet contribution that takes the form: $n\langle \boldsymbol{S}^H \rangle \propto n\zeta U_0 a\langle \boldsymbol{qq} \rangle$.

As a final remark, we have considered average swim forces that are the result of polar order, $\langle \boldsymbol{q} \rangle \neq 0$, as this is the most obvious case. However, what is important is that there is average swim force, $\langle \boldsymbol{F}^{swim} \rangle \neq 0$, not that there is polar order. Recently we have shown[6] that if there is a spatial variation in the intrinsic swim speed $U_0(\boldsymbol{x})$ or reorientation time $\tau_R(\boldsymbol{x})$, as might happen if the local fuel concentration varies, to leading order there is an average swim force: $n\langle \boldsymbol{F}^{swim} \rangle = -\langle \boldsymbol{\sigma}^{swim} \rangle \cdot \nabla \ln(U_0\tau_R)$. This average swim force must then appear in the global force balance (3) or (6) and in the continuum description (7).

Appendix A: the swim force of active matter

There is a recurring discussion in the literature about the nature and origin of the force causing self-propelled bodies to move at low Reynolds number. The discussion revolves about the notion that since self-propulsion is a 'force-free' motion, one cannot say that a self-propelled body experiences a Stokes drag. Or that the propulsive force can be written as a swim force $\boldsymbol{F}^{swim} = \zeta \boldsymbol{U}_0$. And if it is, this swim force is not a 'true' force. However, this is a misunderstanding about what is force-free motion and the nature of hydrodynamics at low Reynolds numbers.

The steady, non-accelerating motion of any body is force-free. At low Reynolds numbers $\mathrm{Re} = \rho U a/\eta \ll 1$, where ρ is the density of the fluid, η is its viscosity, and U and a are the characteristic velocity and length scales of the motion, respectively, the acceleration of the fluid is negligible compared to the viscous and pressure forces and all motion is thus force-free. (We also specify that the inertia of the particle is negligible, which is characterized by the Stokes number $\mathrm{St} = \rho_p/\rho \times \mathrm{Re} \ll 1$, with ρ_p the particle density.) What is meant when one says that self-propulsion at low Reynolds number is force-free is that there is no external force causing the body to move. There are, however, internal forces that cause it to move.

In the simplest description of self propulsion, consider a body of fixed overall shape but whose surface can deform – a 'squirmer'. A paramecium is the classic biological example and phoretic colloidal particles can also be modeled as being propelled by a local slip velocity at their surface.[22,23] At a point $\boldsymbol{x}$ on the surface of a the body, the fluid velocity $\boldsymbol{u}(\boldsymbol{x}) = \boldsymbol{U} + \boldsymbol{\Omega} \times (\boldsymbol{x} - \boldsymbol{X}) + \boldsymbol{u}^s(\boldsymbol{x})$, where $\boldsymbol{u}^s$ is the 'slip' velocity, $\boldsymbol{X}$ is the body center, and $\boldsymbol{U}$ and $\boldsymbol{\Omega}$ are the rigid-body translational and rotational motion of the body about its center. The slip velocity can be expanded in moments $\boldsymbol{u}^s(\boldsymbol{x}') = \boldsymbol{E}^s\cdot\boldsymbol{x}' + \boldsymbol{B}^s:(\boldsymbol{x}'\boldsymbol{x}' - \boldsymbol{I}(x')^2) + \cdots$, where $\boldsymbol{x}' = \boldsymbol{x} - \boldsymbol{X}$, and the tensors $\boldsymbol{E}^s(t)$, $\boldsymbol{B}^s(t)$, *etc.* are, in general, functions of time and are determined by the swimming gait. The linearity of low-Reynolds number or Stokes flow allows a familiar moment expansion[24] of the total hydrodynamic force/torque $\mathscr{F}^H$ on the swimmer

$$\mathscr{F}^H = -\boldsymbol{R}_{\mathscr{F}\mathscr{U}}\cdot\mathscr{U} - \boldsymbol{R}_{\mathscr{F}E}:\boldsymbol{E}^s - \boldsymbol{R}_{\mathscr{F}B} \odot \boldsymbol{B}^s - \cdots, \quad (11)$$

where we have grouped the force/torque together as a single vector in the same fashion as in Stokesian dynamics,[25] $\mathscr{F}^H = (\boldsymbol{F}^H, \boldsymbol{L}^H)$, and similarly for the translational/rotational

velocities: $\mathscr{U} = (\boldsymbol{U},\boldsymbol{\Omega})$. The hydrodynamic resistance tensors $\boldsymbol{R}_{\mathscr{F}\mathscr{U}}$, $\boldsymbol{R}_{\mathscr{F}E}$, *etc.* are functions of the body geometry only and couple the force to the velocity, to the 'squirming set' $\boldsymbol{E}^{\mathrm{s}}(t)$, $\boldsymbol{B}^{\mathrm{s}}(t)$, *etc.*

In the Stokes flow regime, the rigid body's motion is overdamped and thus force-free: $\mathscr{F}^{\mathrm{H}} + \mathscr{F}^{\mathrm{ext}} = 0$, where $\mathscr{F}^{\mathrm{ext}}$ is any external force such as gravity or an external torque. For a passive (*i.e.* non-swimming or non-active) body when $\mathscr{F}^{\mathrm{ext}} = 0$, $\mathscr{F}^{\mathrm{H}} = 0$ and there is no motion. For a swimmer when $\mathscr{F}^{\mathrm{ext}} = 0$, $\mathscr{F}^{\mathrm{H}} = 0$ is still true, but $\mathscr{U} \neq 0$ in (11) – the drag, $-\boldsymbol{R}_{\mathscr{F}\mathscr{U}}\cdot\mathscr{U}$, cancels the swimming part, $-\boldsymbol{R}_{\mathscr{F}E}:\boldsymbol{E}^{\mathrm{s}} - \boldsymbol{R}_{\mathscr{F}B} \odot \boldsymbol{B}^{\mathrm{s}} - \cdots$. Indeed, we can define

$$\mathscr{F}^{\mathrm{swim}} = -\boldsymbol{R}_{\mathscr{F}\mathrm{E}}:\boldsymbol{E}^{\mathrm{s}} - \boldsymbol{R}_{\mathscr{F}\mathrm{B}} \odot \boldsymbol{B}^{\mathrm{s}} - \cdots, \tag{12}$$

and

$$\mathscr{F}^{\mathrm{drag}} = -\boldsymbol{R}_{\mathscr{F}\mathscr{U}}\cdot\mathscr{U}, \tag{13}$$

and then the required force-free motion $\mathscr{F}^{\mathrm{H}} = \mathscr{F}^{\mathrm{drag}} + \mathscr{F}^{\mathrm{swim}} = 0$ gives

$$\mathscr{U} = \boldsymbol{R}_{\mathscr{F}\mathscr{U}}{}^{-1}\cdot\mathscr{F}^{\mathrm{swim}}. \tag{14}$$

Eqn (12) is the definition of the swim force (and torque). The reorientation of a nonBrownian swimmer that gives rise to its random walk arises from the squirming set $\boldsymbol{E}^{\mathrm{s}}(t)$, *etc.* changing direction (relative to the body fixed coordinate system). That the swim force is a real measurable force can be appreciated by recognizing that if one wanted to keep the swimmer from moving, the force required is $\boldsymbol{F}^{\mathrm{swim}}$.

We have considered the simplest model for self-propulsion, namely a squirmer. However, as shown by Swan *et al.*[26] the exact same structure applies for swimmers that propel by large deformations of their body shape – the hydrodynamic resistance tensors are now also functions of time but the definitions, (11)–(13), apply at each instant.

It is important to note that a nonzero swim force does not imply that the fluid velocity disturbance caused by the swimmer decays as $1/r$ as it would for a body with a nonzero hydrodynamic force. This is most clearly seen from the integral representation for the solution to the Stokes equations. The velocity field outside a particle in Stokes flow can be expanded in force moments to give

$$\begin{aligned} u_i(\boldsymbol{x}) \;=\; & -J_{ij}F_j^{\mathrm{H}} - \frac{1}{2}\varepsilon_{ijk}\nabla_k J_{il}L_j^{\mathrm{H}} \\ & - \frac{1}{2}\left(\nabla_k J_{ij} + \nabla_j J_{ik}\right)S_{jk}^{\mathrm{H}} \\ & - \frac{1}{2}\nabla_j\nabla_k J_{il}Q_{jkl}^{\mathrm{H}} - \cdots, \end{aligned} \tag{15}$$

where the Stokeslet, $8\pi\eta J_{ij}(\boldsymbol{x}) = \delta_{ij}/r + x_i x_j/r^3$, is evaluated at the particle center. The hydrodynamic force and torque are given by their usual expressions: $\boldsymbol{F}^{\mathrm{H}} = \int\sigma\cdot\boldsymbol{n}\mathrm{d}S$, $\boldsymbol{L}^{\mathrm{H}} = \int\boldsymbol{x}'\times\sigma\cdot\boldsymbol{n}\mathrm{d}S$, and the stresslet is given by $\boldsymbol{S}^{\mathrm{H}} = \frac{1}{2}\int[\boldsymbol{x}'\sigma\cdot\boldsymbol{n} + \sigma\cdot\boldsymbol{n}\boldsymbol{x}' - 2\eta(\boldsymbol{u}^{\mathrm{s}}\boldsymbol{n} + \boldsymbol{n}\boldsymbol{u}^{\mathrm{s}})]\mathrm{d}S$, with $\boldsymbol{\sigma}$ the fluid stress tensor; there is a corresponding expression for the hydrodynamic quadrupole $\boldsymbol{Q}^{\mathrm{H}}$, *etc.*

Since the drag force $\mathscr{F}^{\mathrm{drag}}$ balances the swim force there is no hydrodynamic force or torque on the swimmer: $\mathscr{F}^{\mathrm{H}} = 0$ ($\boldsymbol{F}^{\mathrm{H}} = 0$, $\boldsymbol{L}^{\mathrm{H}} = 0$), and the velocity disturbance decays at leading order as $1/r^2$ coming from the stresslet $\boldsymbol{S}^{\mathrm{H}}$. If the slip velocity does not generate a stresslet, then the leading order velocity disturbance decays as $1/r^3$ corresponding to the quadrupole $\boldsymbol{Q}^{\mathrm{H}}$. And so on depending on the nature of the propulsive mechanism and the body geometry. There is no difficulty (or ambiguity) in speaking about a swim force and a drag force for a self-propelled body and the velocity disturbance generated by the swimming body decaying faster than $1/r$. In fact, Blake[22] and Ishikawa *et al.*[27] expanded the hydrodynamic interactions between two squirmers in a series of surface radial and tangential velocity modes. These modes may cancel such that the velocity disturbance decays as $1/r^n$, which can be very fast for large n.

Even for a single particle, hydrodynamics can also generate a single particle contribution to the active stress $\boldsymbol{\sigma}_{\mathrm{h}} \sim n\zeta U_0 a\langle\boldsymbol{q}\boldsymbol{q}\rangle$, which scales as $n\zeta U_0 a$, as opposed to the swim stress that scales as $n\zeta {U_0}^2\tau_{\mathrm{R}}$. As discussed by Takatori *et al.*[5] for fast swimmers ($\mathrm{Pe}_{\mathrm{R}} \to 0$), $\boldsymbol{\sigma}_{\mathrm{h}}/\boldsymbol{\sigma}^{\mathrm{swim}} \sim U_0 a/({U_0}^2\tau_{\mathrm{R}}) = a/(U_0\tau_{\mathrm{R}}) = \mathrm{Pe}_{\mathrm{R}} \to 0$.

Considering other forces that affect the motion of active particles, the overdamped Langevin equation of a set of swimmers can be written as,

$$0 = \mathscr{F}^{\mathrm{drag}} + \mathscr{F}^{\mathrm{swim}} + \mathscr{F}^{\mathrm{B}} + \mathscr{F}^{\mathrm{ext}} + \mathscr{F}^{\mathrm{P}}, \tag{16}$$

where $\mathscr{F}^{\mathrm{B}} = 2k_{\mathrm{B}}T\boldsymbol{R}_{\mathscr{F}\mathscr{U}}\delta(t)$ is a Brownian force with zero mean, $\mathscr{F}^{\mathrm{ext}}$ is any external force, and $\mathscr{F}^{\mathrm{P}}$ is a particle–particle interactive or collision force. The resistance tensors are now functions of both the individual swimmer body shape and the relative separation and orientation of all the swimmers, as is standard in Stokesian dynamics.

In the simplest case where the hydrodynamic interactions among the swimmers are neglected and only translational swimming is relevant, the hydrodynamic resistance tensor $\boldsymbol{R}_{\mathscr{F}\mathscr{U}}$ can be simplified to an isotropic drag tensor $\zeta\boldsymbol{I}$, so that $\boldsymbol{F}^{\mathrm{drag}} = -\zeta\boldsymbol{U}$, $\boldsymbol{F}^{\mathrm{swim}} = \zeta U_0\boldsymbol{q}$, and we have the 'Active Brownian Particle' (ABP) model eqn (2) of the main text. Here, $\boldsymbol{q}(t)$ is the orientation vector for the swimming direction and is subject to run-and-tumble motion or rotational Brownian diffusion, which are equivalent,[19] and comes from the torque balance in (16). For a spherical swimmer, $\zeta = 6\pi\eta a$ and the swim force arises from the quadrupole squirming set $\boldsymbol{B}^{\mathrm{s}}(t)$.

In this work we focus on this ABP model, with both translational (D_{T}) and rotational (D_{R}) diffusivity. In this case the time scale is set by $1/D_{\mathrm{R}}(= \tau_{\mathrm{R}})$, and the reorientation Péclet number[5] $\mathrm{Pe}_{\mathrm{R}} = aD_{\mathrm{R}}/U_0 = a/\ell$ controls how far the swimmer travels in one reorientation time – its run length $\ell = U_0\tau_{\mathrm{R}}$ – compared to its size a. The ratio $D_{\mathrm{T}}/(a^2D_{\mathrm{R}})$ controls the relative strength of translational Brownian diffusion and reorientational diffusion.

With $\mathscr{F}^{\mathrm{swim}}$ defined in (12), the suspension stress[28,29] in the absence of macroscopic shearing and external torques is:

$$\langle\boldsymbol{\sigma}\rangle = -\langle p_{\mathrm{f}}\rangle\boldsymbol{I} + \langle\boldsymbol{\sigma}^{\mathrm{swim}}\rangle + \langle\boldsymbol{\sigma}^{\mathrm{B}}\rangle + \langle\boldsymbol{\sigma}^{\mathrm{P}}\rangle, \tag{17}$$

where $-\langle p_{\mathrm{f}}\rangle\boldsymbol{I}$ is the isotropic (incompressible) fluid pressure, $\langle\boldsymbol{\sigma}^{\mathrm{swim}}\rangle$ is the swim stress, $\langle\boldsymbol{\sigma}^{\mathrm{B}}\rangle = -nk_{\mathrm{B}}T\boldsymbol{I}$ is the Brownian stress,[29]

and $\langle \boldsymbol{\sigma}^{\mathrm{P}} \rangle$ is the particle collision stress. The swim stress $\langle \boldsymbol{\sigma}^{\mathrm{swim}} \rangle$ can be anisotropic if the swimmers' reorienting process is biased by, for example, an external torque. For the ABP model, $\langle \boldsymbol{\sigma}^{\mathrm{swim}} \rangle$ has been thoroughly discussed in both the isotropic[5] and anisotropic[8] cases. In the text, we have written the 'particle stress' $\langle \boldsymbol{\sigma}^{(\mathrm{p})} \rangle = \langle \boldsymbol{\sigma}^{\mathrm{swim}} \rangle + \langle \boldsymbol{\sigma}^{\mathrm{B}} \rangle + \langle \boldsymbol{\sigma}^{\mathrm{P}} \rangle$ as is customary in colloidal dynamics.

Appendix B: anisotropic stress under $\hat{H}$ field

In this section we follow the convention of Frankel and Brenner[30] to derive the anisotropic swim diffusivity $\boldsymbol{D}^{\mathrm{swim}}$ and ideal gas swim stress $\boldsymbol{\sigma}^{\mathrm{swim}} = -n\zeta \boldsymbol{D}^{\mathrm{swim}}$. Similar methods have also been used in Zia and Brady[31] and Takatori and Brady.[8] In Frankel and Brenner's theory $\boldsymbol{q}$ is a local degree of freedom. For the swimmers considered here, $\boldsymbol{q}$ is the orientation vector of each swimmer. The steady state distribution, $P_0^{\infty}(\boldsymbol{q})$, is analytically solvable from the Langevin equation for $\boldsymbol{q}$:

$$\frac{\mathrm{d}\boldsymbol{q}}{\mathrm{d}t} = \Omega_{\mathrm{c}} \boldsymbol{q} \times \hat{\boldsymbol{H}} + \dot{\eta}, \tag{18}$$

where $\hat{\boldsymbol{H}}$ is the unit vector in the direction of the orienting field, Ω_{c} is its magnitude, and $\dot{\eta}$ is the rotational Brownian motion characterized by D_{R}.

The orientation-average velocity is defined as:

$$\langle \boldsymbol{U} \rangle = \int_{\boldsymbol{q}} P_0^{\infty}(\boldsymbol{q}) \boldsymbol{U}(\boldsymbol{q}) \mathrm{d}\boldsymbol{q}. \tag{19}$$

By decomposing $\Delta \boldsymbol{U}(\boldsymbol{q}) = \boldsymbol{U}(\boldsymbol{q}) - \langle \boldsymbol{U} \rangle$, the effective diffusivity is given by

$$\boldsymbol{D}^{\mathrm{swim}} = \int_{\boldsymbol{q}} P_0^{\infty}(\boldsymbol{q}) \boldsymbol{B}(\boldsymbol{q}) \Delta \boldsymbol{U}(\boldsymbol{q}) \mathrm{d}\boldsymbol{q}, \tag{20}$$

where the $\boldsymbol{B}$ field is the solution to

$$\nabla_{\boldsymbol{q}} \cdot [\boldsymbol{u} P_0^{\infty} \boldsymbol{B} - \boldsymbol{d} \cdot \nabla_{\boldsymbol{q}} (P_0^{\infty} \boldsymbol{B})] = \Delta \boldsymbol{U} P_0^{\infty}, \tag{21}$$

$$\int_{\boldsymbol{q}} P_0^{\infty} \boldsymbol{B} \mathrm{d}\boldsymbol{q} = 0, \tag{22}$$

with appropriate BC in $\boldsymbol{q}$ space. Here $\boldsymbol{u}$ and $\boldsymbol{d}$ are velocity and (intrinsic) diffusivity in $\boldsymbol{q}$ space, respectively. For swimmers in this work, $\boldsymbol{u}$ is the torque applied by the $\hat{\boldsymbol{H}}$ field, and $\boldsymbol{d} = D_{\mathrm{R}} \boldsymbol{I}$ is the rotational diffusivity.

In a 2D system, $\boldsymbol{q} = (\cos\theta, \sin\theta)$, and we define $\hat{\boldsymbol{H}} = (0,1)$. The steady probability distribution $P_0^{\infty}(\theta)$ is:

$$P_0^{\infty}(\theta) = \frac{\exp(-\chi_{\mathrm{R}} \cos\theta)}{\pi I_0(\chi_{\mathrm{R}})}, \tag{23}$$

and the average orientation is

$$\langle q_z \rangle = \frac{I_1(\chi_{\mathrm{R}})}{I_0(\chi_{\mathrm{R}})}, \tag{24}$$

where $\chi_{\mathrm{R}} = \Omega_{\mathrm{c}} \tau_{\mathrm{R}} = \Omega_{\mathrm{c}} / D_{\mathrm{R}}$, and I_0, I_1, I_n, ... are Bessel functions.

With the mathematical expansion

$$\exp(z\cos\theta) = I_0(z) + 2\sum_{n=1}^{\infty} I_n(z)\cos(n\theta), \tag{25}$$

we have

$$D_{\perp}^{\mathrm{swim}} = 2\sum_{n=1}^{\infty} \frac{I_n(\chi_{\mathrm{R}})}{n\chi_{\mathrm{R}} I_0(\chi_{\mathrm{R}})} \times \int_{-\pi}^{\pi} \frac{\exp(-\chi_{\mathrm{R}}\cos\theta)\sin\theta\sin(n\theta)}{2\pi I_0(\chi_{\mathrm{R}})} \mathrm{d}\theta. \tag{26}$$

The parallel diffusivity, $D_{\parallel}^{\mathrm{swim}}$, is more complicated. First define

$$\begin{aligned} f(p) \;=\; & -(p+\pi) I_1(\chi_{\mathrm{R}}) - \sin p I_0(\chi_{\mathrm{R}}) \\ & + I_1(\chi_{\mathrm{R}}) \left(p + \pi + 2\frac{I_1(\chi_{\mathrm{R}})\sin p}{I_0(\chi_{\mathrm{R}})} + \cos p \sin p \right) \\ & + \sum_{n=2}^{\infty} I_n(-\chi_{\mathrm{R}}) \left(-\frac{I_1(\chi_{\mathrm{R}})\sin(np)}{n I_0(\chi_{\mathrm{R}})} \right. \\ & \left. + \frac{\cos(np)\sin p - n\cos p \sin(np)}{n^2 - 1} \right) \end{aligned} \tag{27}$$

and

$$B_{\parallel}(\theta) = \int_{-\pi}^{\theta} \exp(\chi_{\mathrm{R}} \cos p) f(p) \mathrm{d}p. \tag{28}$$

Finally,

$$D_{\parallel}^{\mathrm{swim}} = \int_{-\pi}^{\pi} \left(\cos\theta + \frac{I_1(\chi_{\mathrm{R}})}{I_0(\chi_{\mathrm{R}})} \right) \times \frac{\exp(-\chi_{\mathrm{R}}\cos\theta)}{2\pi I_0(\chi_{\mathrm{R}})} B_{\parallel}(\theta) \mathrm{d}\theta. \tag{29}$$

These expressions are used for the anisotropic swim stress in the text.

Appendix C: solution of continuum eqn (7)

The solution of the continuum eqn (7) at steady state requires a constitute law: $\langle \boldsymbol{\sigma}^{(\mathrm{p})} \rangle (\phi, U_0, D_{\mathrm{T}}, \tau_{\mathrm{R}})$. For the results in Fig. 2, the constitutive law can be found in the work of Takatori and Brady.[6] For the results in Fig. 5, $k_{\mathrm{s}} T_{\mathrm{s}} \ll k_{\mathrm{B}} T$ since U_0 is small, and therefore the stress for passive Brownian particles in 2D[32] is used: $\langle \boldsymbol{\sigma}^{(\mathrm{p})} \rangle (\phi, U_0, D_{\mathrm{T}}, \tau_{\mathrm{R}}) \propto 1/(1-\phi)^2$.

Acknowledgements

This work was supported by NSF Grant No. CBET 1437570.

References

1 R. Wittkowski, A. Tiribocchi, J. Stenhammar, R. J. Allen, D. Marenduzzo and M. E. Cates, *Nat. Commun.*, 2014, **5**, 4351.
2 J. Stenhammar, A. Tiribocchi, R. J. Allen, D. Marenduzzo and M. E. Cates, *Phys. Rev. Lett.*, 2013, **111**, 145702.
3 M. E. Cates and J. Tailleur, *Annu. Rev. Condens. Matter Phys.*, 2015, **6**, 219–244.

4 A. M. Menzel and H. Löwen, *Phys. Rev. Lett.*, 2013, **110**, 055702.
5 S. C. Takatori, W. Yan and J. F. Brady, *Phys. Rev. Lett.*, 2014, **113**, 028103.
6 S. C. Takatori and J. F. Brady, *Phys. Rev. E: Stat., Nonlinear, Soft Matter Phys.*, 2015, **91**, 032117.
7 M. Hennes, K. Wolff and H. Stark, *Phys. Rev. Lett.*, 2014, **112**, 238104.
8 S. C. Takatori and J. F. Brady, *Soft Matter*, 2014, **10**, 9433.
9 J. Tailleur and M. E. Cates, *Europhys. Lett.*, 2009, **86**, 60002.
10 E. Lushi, R. E. Goldstein and M. J. Shelley, *Phys. Rev. E: Stat., Nonlinear, Soft Matter Phys.*, 2012, **86**, 040902.
11 J. Stenhammar, D. Marenduzzo, R. J. Allen and M. E. Cates, *Soft Matter*, 2014, **10**, 1489.
12 A. Lefauve and D. Saintillan, *Phys. Rev. E: Stat., Nonlinear, Soft Matter Phys.*, 2014, **89**, 021002.
13 S. Li, H. Jiang and Z. Hou, *Soft Matter*, 2015, DOI: 10.1039/C5SM00768B.
14 X. Yang, M. L. Manning and M. C. Marchetti, *Soft Matter*, 2014, **10**, 6477.
15 S. A. Mallory, A. Šarić, C. Valeriani and A. Cacciuto, *Phys. Rev. E: Stat., Nonlinear, Soft Matter Phys.*, 2014, **89**, 052303.
16 Y. Fily, A. Baskaran and M. F. Hagan, *Soft Matter*, 2014, **10**, 5609–5617.
17 A. P. Solon, J. Stenhammar, R. Wittkowski, M. Kardar, Y. Kafri, M. E. Cates and J. Tailleur, *Phys. Rev. Lett.*, 2015, **114**, 198301.
18 A. P. Solon, Y. Fily, A. Baskaran, M. E. Cates, Y. Kafri, M. Kardar and J. Tailleur, *arXiv:cond-mat/1412.3952*, 2014.
19 M. E. Cates and J. Tailleur, *Europhys. Lett.*, 2013, **101**, 20010.
20 W. Yan and J. F. Brady, 2015, in preparation.
21 M. Enculescu and H. Stark, *Phys. Rev. Lett.*, 2011, **107**, 058301.
22 J. R. Blake, *J. Fluid Mech.*, 1971, **46**, 199–208.
23 J. L. Anderson, *Annu. Rev. Fluid Mech.*, 1989, **21**, 61–99.
24 S. Kim and S. J. Karrila, *Microhydrodynamics: Principles and Selected Applications*, Courier Corporation, 2005.
25 L. Durlofsky, J. F. Brady and G. Bossis, *J. Fluid Mech.*, 1987, **180**, 21–49.
26 J. W. Swan, J. F. Brady, R. S. Moore and ChE 174, *Phys. Fluids*, 2011, **23**, 71901.
27 T. Ishikawa, M. P. Simmonds and T. J. Pedley, *J. Fluid Mech.*, 2006, **568**, 119–160.
28 G. K. Batchelor, *J. Fluid Mech.*, 1970, **41**, 545.
29 J. F. Brady, *J. Chem. Phys.*, 1993, **98**, 3335–3341.
30 I. Frankel and H. Brenner, *J. Fluid Mech.*, 1989, **204**, 97–119.
31 R. N. Zia and J. F. Brady, *J. Fluid Mech.*, 2010, **658**, 188–210.
32 E. Helfand, H. L. Frisch and J. L. Lebowitz, *J. Chem. Phys.*, 1961, **34**, 1037–1042.